Microelectronics Reliability 55 (2015) 1384–1390

Contents lists available at ScienceDirect

Microelectronics Reliability

journal homepage: www.elsevier.com/locate/mr

Envelope probability and EFAST-based sensitivity analysis method for electronic prognostic uncertainty quantification

Bo Sun [a,b], Wuyang Pan [a,*], Zili Wang [a], Kam-Chuen Yung [b]

[a] School of Reliability and Systems Engineering, Beihang University (BUAA), No. 37 XueYuan Rd, Haidian, Beijing 100191, China
[b] PCB Technology Center, Department of Industrial and Systems Engineering, The Hong Kong Polytechnic University, Hung Hom, Hong Kong

ARTICLE INFO

Article history:
Received 25 May 2015
Received in revised form 17 June 2015
Accepted 25 June 2015
Available online 14 July 2015

Keywords:
Sensitivity analysis
Uncertainty
Electronic
Prognostic
EFAST
Envelope-probability

ABSTRACT

The primary phase of electronic prognostic uncertainty quantification included the identification and quantification of uncertainty sources through utilizing sensitivity analysis method. An improved EFAST-based sensitivity analysis method that considered the possibility of parameter fluctuation was used to identify the key factors (KFS) of uncertainty sources. Also, an envelope probability method was adopted to further quantify the key factors of parameter distribution. Finally, a board-level electronic product was chosen as the study case of this paper. Comparing the result of uncertainty quantification, sensitivity analysis was used to drive the result of the single-dimensional method. It was obvious that the sensitivity analysis method used in this paper has optimized the input parameters of the model and improved the accuracy of electronic prognostic uncertainty quantification.

1. Introduction

The uncertainties in the process of prognostic could affect the applicability of prognostics methods and the credibility of prognostics results [1]. Therefore, various approaches had been proposed to analyse and quantify the uncertainty during the prediction process. Uncertainty quantification is a process of depicting, estimating and analysing many uncertain factors in the system [2]. The identification and quantification of uncertainty sources were an initial and important stage of uncertainty quantification, since the model inputs were generated by them. Sensitivity analysis, as an effective method could be used in the initial stage of uncertainty quantification. Thus, the input parameters of the model could be optimized by sensitivity analysis [3]. In this analysis, the uncertainty of model output was allocated to the key factors selected from different input parameters (KFS, which caused the output uncertainty of the model) [4].

The identification and quantification of uncertainty sources had been studied in several papers. Ba-Ngu Vo et al. [5] adopted a sequential Monte Carlo method to obtain the prediction result with higher accuracy. Sankararaman et al. [6] explained the application of Bayesian network approach in uncertainty problems. The sensitivity analysis had already been widely applied in uncertainty quantification. Helton et al. [7] proposed an uncertainty quantification method combined with sensitivity analysis. Andre [8] held that the sensitivity analysis, similar as uncertainty analysis, could reveal or find the causes of output uncertainty. The sensitivity analysis was employed to find the contribution of each input parameter to the changes of system output in a number of researches [9,10]. Helton and Davis [11] summarized the expressions of various input sensitivity parameters and calculation methods.

As a global sensitivity method proposed by Saltelli et al. [12], the EFAST (Extended Fourier Amplitude Sensitivity Test) is of high precision. However, the probability of parameter fluctuation had not been taken account in this method for the identification of uncertainty sources. Though Hammonds et al. [13] figured out the distribution types which different uncertainty parameters followed, there was still uncertainty in distribution parameters. A method based on envelope-probability was proposed by Ferson and Troy Tucker, aiming to remove both the random uncertainty and the cognitive uncertainty [14]. The cognitive uncertainty was denoted as the distribution types and parameters. However, there were still some problems in the previous research. The possibility of weighing parameters in sensitivity analysis had not been considered, and the parameters in the distribution followed by KFS had not been defined clearly.

In this paper, an enhanced sensitivity analysis approach was proposed to improve the accuracy of the model input. Through combining the fluctuation percentage of uncertainty quantification and the probability of parameter fluctuation, the EFAST method was adopted to identify KFS in the identification of uncertainty sources. The envelope-probability

* Corresponding author.
E-mail addresses: sunbo@buaa.edu.cn (B. Sun), panwuyang@buaa.edu.cn (W. Pan), wzl@buaa.edu.cn (Z. Wang), wincokc.yung@polyu.edu.hk (K.-C. Yung).

http://dx.doi.org/10.1016/j.microrel.2015.06.115

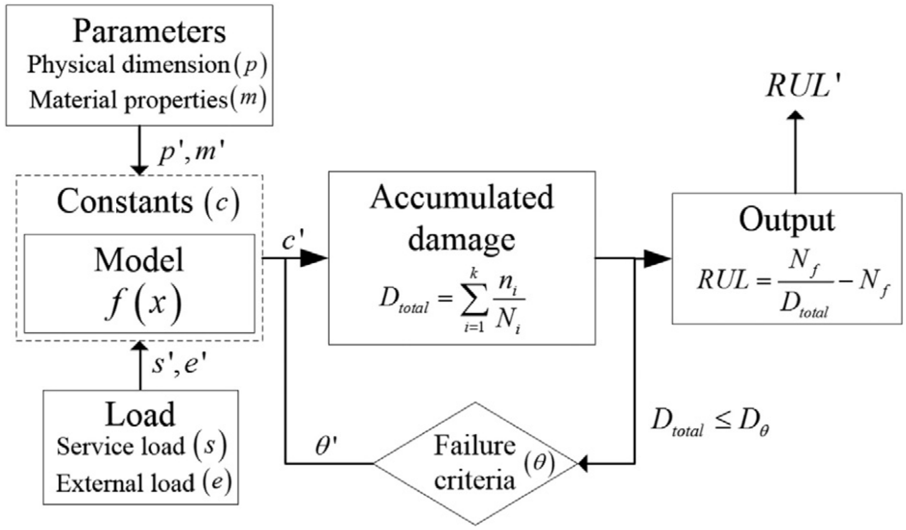

Fig. 1. Uncertainty propagation in RUL prognostics.

method is also used to obtain the probability distribution of KFS, which achieved pre-defined accuracy. Simulations of a board-level electronic product (contains 49 kinds of device type, 161 components) was conducted to validate the effectiveness of such a hybrid approach in comparison with the original method. The results of the simulation showed that such enhanced sensitivity analysis had obviously improved the accuracy of uncertainty quantification.

2. RUL prognostic and uncertainty propagation

For the electronic products, physics-of-failure (PoF)-based methods was shown to be effective for prognostic [15]. The uncertainty propagation in the process of electronic prognostics can be described as Fig. 1.

$p = \{p_1, p_2 \cdots p_n\}$ in Fig. 1 refers to the physical dimension like length, width, height and so on. $m = \{m_1, m_2 \cdots m_n\}$ is the material properties such as Poisson's ratio and Young's modulus. $s = \{s_1, s_2 \cdots s_n\}$ is the service load like the voltage or current caused by the operation of the product itself. And $e = \{e_1, e_2 \cdots e_n\}$ refers to the external load, such as temperature and vibration.

$$N_f = f(p, m, s, e, c) \tag{1}$$

The accumulated damage percentage D_{total} can be expressed as follows:

$$D_{total} = \sum_{i=1}^{k} D_i = \sum_{i=1}^{k} \frac{n_i}{N_i}. \tag{2}$$

The failure criterion is θ.

$$D_{total} \le D_\theta \tag{3}$$

Table 1
The weight of parameters.

Weight (k)	Meaning
1	More likely to happen
0.5	Likely to happen
0	Not likely to happen

Through the output of uncertainty propagation N_f, the remaining useful lifetime (RUL) can be calculated as follows:

$$RUL = \frac{N_f}{D_{total}} - N_f. \tag{4}$$

The uncertainty parameters are p', m', s', e', c', and θ'. The outputs value with uncertainty, RUL' can be described as a series of statistical eigenvalues by uncertainty propagation.

3. Sensitivity analysis approach

3.1. Sensitivity analysis of uncertainty source identification

3.1.1. Joint parameter impact

Since a single parameter fluctuation will be affected by other parameters, the impacts were reflected in the process of EFAST based the sensitivity analysis method. If the model is $y = f(x)$, where the input is $x = (x_1, x_2 \ldots x_n)$, y is the output value. The model with total fluctuation percentage $F(y)$ can be decomposed as follows:

$$F(y) = \sum_i F_i + \sum_{i \ne j} F_{ij} + \sum_{i \ne j \ne m} F_{ijm} + F_{12\ldots k} \tag{5}$$

where i, j, and m are corresponding to the serial number of different KFS and range from 1 to k. F_i is the fluctuation percentage of the results for a single changed factor. The multi-fluctuation percentage F_{ij} generated by x_i, x_j to the final results y can be calculated as follows:

$$F_{ij} = \left| F_i \cdot F_j - F_i - F_j \right|. \tag{6}$$

3.1.2. Possibility of parameter uncertainty

The possibility of parameter uncertainty was introduced to the sensitivity analysis as the probability of each parameter fluctuation is different. The weight of each parameter in sensitivity analysis is defined in Table 1.

Table 2
Distribution type of parameters.

p' ~ Triangle	s' ~ Normal	θ' ~ Normal
m' ~ Triangle	e' ~ Normal	c' ~ Uniform

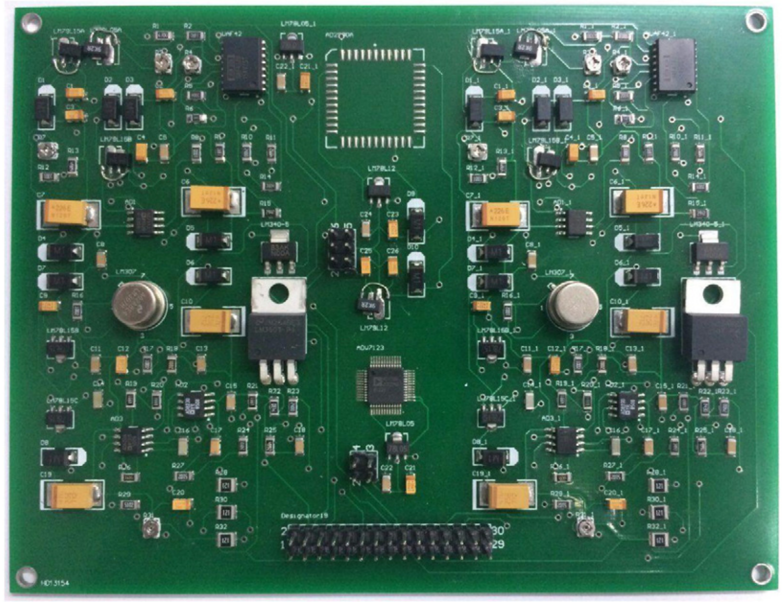

Fig. 2. The strain test board.

The comprehensive weight of multiple factors can be shown as follows:

$$k_{ij} = k_i \cdot k_j \tag{7}$$

where i and j refer to different KFS and range from 1 to k.

3.1.3. Parameter sorting

The sensitivity index is S. The first-order sensitivity index of x_i is S_i, combing with k, which can be defined as follows:

$$S_i = \frac{k_i \cdot F_i}{F}. \tag{8}$$

Similarly, the parameter sensitivity index of the 2nd-order and the 3rd-order can be defined as follows:

$$S_{ij} = \frac{k_{ij} \cdot F_{ij}}{F}, \ S_{ijm} = \frac{k_{ijm} \cdot F_{ijm}}{F}. \tag{9}$$

The influence between parameters can be described as S_{T_i} which is the amount of each order index.

$$S_{T_i} = S_i + S_{ij} + S_{ijm} + \cdots + S_{12\cdots i \cdots k} \tag{10}$$

where the total sensitivity index of x_i is S_{T_i}; the 1st order to the k-order sensitivity index of x_i is S_i to $S_{12 \cdots i \cdots k}$.

3.2. Sensitivity analysis of uncertainty source quantification

3.2.1. Distribution of parameters

All the parameters by the rules were proposed in the literature [13]. The distribution type that $X_i = \{p', m', s', e', c', \theta'\}$ followed is shown in Table 2.

Table 3
External load conditions.

Load conditions	Value
Temperature range	−45 °C to 125 °C
High/low temperature dwell time	10 min
The rate of temperature variation	15 °C/min
Time of a cycle	42.6 min
The frequency of the cycle	10 cycles

3.2.2. Sensitivity analysis of distribution parameters

If more than two probability envelope areas are calculated, the other uncertainty factors will all follow the given envelope-probability [14]:

$$\Delta s_i = (area(B) - area(T_i))/area(B) \times 100\% \tag{11}$$

where $area(B)$ is the probability envelope area of the output y when the uncertainty of distribution parameters have not been removed; $area(T_i)$ is the uncertainty part of distribution parameters d_i; Δs_i is the sensitivity index of distribution parameter x_i. The step of the envelope-probability-based method is in detail can be described as follows:

Step 1: Describing all the KFS by the probability envelope and then calculating the total probability envelope $area(B)$.

Step 2: Extracting 3 ~ 5 groups (depends on the demanded accuracy) of distribution parameters in the range of selected factors to describe ten precision distributions of selected factors. When the selected factors followed different precision distribution and other uncertainty factors are in the given probability envelope (same as Step 1),the total $area(T_i)$ can be calculated corresponding to each group of the parameters.

Step 3: Using Eq. (11) to calculate the Δs_i of each distribution parameter.

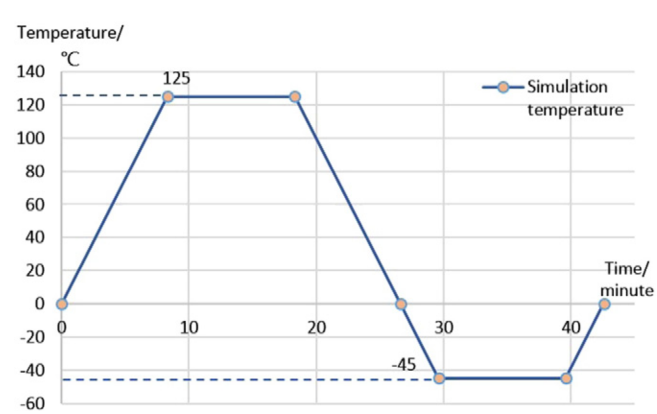

Fig. 3. Ambient temperature load profile.

Table 4
Sensitivity analysis of the solder joint thermal fatigue.

Parameters	Average	k	Range	S_T	New (origin) ranking
ε_f	0.325	1	42.77%	0.1751	2 (4)
c	0.6	0.5	13.24%	0.0818	4 (5)
A	0.15	0	116%	0	5 (1)
h	0.5	1	84.5%	0.2159	1 (2)
L_D	7.14	0.5	71.7%	0.1256	3 (3)

Table 5
Sensitivity analysis of the PTH.

Parameters	Average	k	Range	S_T	New (origin) ranking
R	0.3	0.5	85.43%	0.0824	4 (2)
l	0.5	1	70.02%	0.1594	2 (3)
t	0.25	1	98.56%	0.1923	1 (1)
E_{Cu}	1300	0.5	12.35%	0.1107	3 (4)
D_f	0.6	0	11.63%	0	5 (5)

Table 6
Sensitivity analysis of the electro migration.

Parameters	Average	k	Range	S_T	New (origin) ranking
j	3.25	1	42.77%	0.1745	3 (3)
c	−0.6	0.5	13.24%	0.1291	4 (5)
A	0.25	0	29.9%	0	5 (4)
W	0.1	0.5	117.3%	0.2154	2 (1)
d	0.6	1	116.5%	0.2845	1 (2)

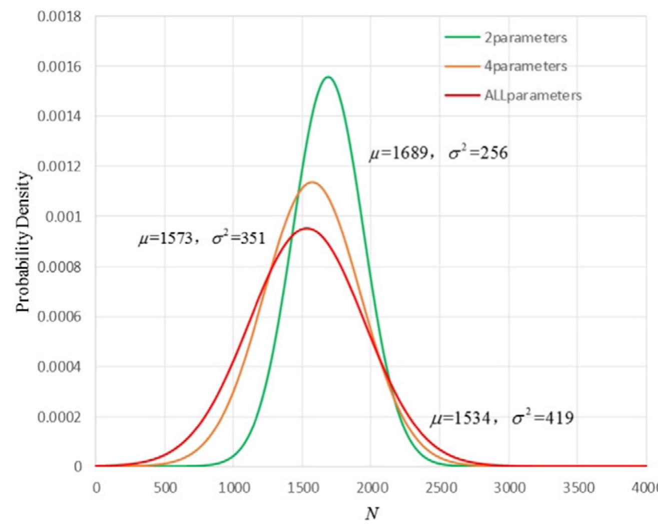

Fig. 5. The effects of different quantity of KFS.

4. Case study

4.1. Case description

A two-channel static strain test boards was selected as a typical case in this paper. The board contained 49 kinds of devices and 161 components in total which is shown in Fig. 2.

4.2. Prognostic model

The failure of the mechanism model was caused by those components as mentioned above: solder thermal fatigue model [16] (Coffin–Manson), plated-through-hole thermal fatigue model [17] (PTH) and electro-migration model [18] (Black). The predictive linear cumulative damage models [19] and failure mechanism competition model [20] should be concluded in the whole process.

4.3. Loading conditions

The external loads that this case suffered in the process of the simulation are shown in Table 3, and the ambient temperature load profile is defined in Fig. 3.

The case had been under the conditions of present experiment for 50 days before the fault prediction began.

4.4. Sensitivity analysis

4.4.1. Identification of uncertainty sources

According to Eqs. (5)–(10), the KFS can be identified from the uncertainty sources through the improved EFAST-based sensitivity analysis.

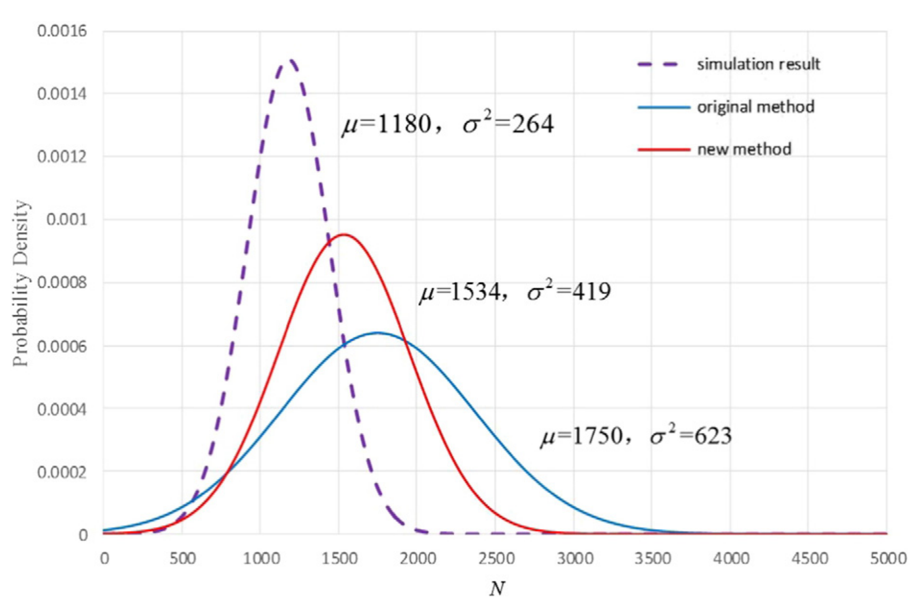

Fig. 4. The results of the two sensitivity analysis method.

Table 7
Distribution type and range of the parameters.

Parameters	Range of the parameters		
$\varepsilon_f \sim N$	$u \sim [0.28, 0.35]$		$\sigma^2 = 0.25$
$E_{Cu} \sim N$	$u \sim [1100, 1500]$		$\sigma^2 = 450$
$d \sim N$	$u \sim [0.5, 0.7]$		$\sigma^2 = 0.6$
$L_D \sim U$	$Lb \sim [0.62, 0.7]$		$Ub \sim [0.72, 0.8]$
$t \sim U$	$Lb \sim [0.1, 0.2]$		$Ub \sim [0.3, 0.4]$
$l \sim U$	$Lb \sim [0.3, 0.5]$		$Ub \sim [0.6, 0.8]$
$W \sim U$	$Lb \sim [0.05, 0.08]$		$Ub \sim [0.12, 0.14]$
$h \sim T$	$Lb \sim [0.3, 0.6]$	$M \sim [0.5, 0.8]$	$Ub \sim [0.8, 1.0]$
$j \sim T$	$Lb \sim [2.4, 2.8]$	$M \sim [3.2, 3.6]$	$Ub \sim [3.5, 4.0]$

Table 8
The values of the KFS.

ε_f		L_D	
$u = 0.28$	$\sigma^2 = 0.25$	$Lb = 0.62$	$Ub = 0.72$
$u = 0.32$	$\sigma^2 = 0.25$	$Lb = 0.66$	$Ub = 0.76$
$u = 0.35$	$\sigma^2 = 0.25$	$Lb = 0.70$	$Ub = 0.80$

h		
$Lb = 0.3$	$M = 0.5$	$Ub = 0.8$
$Lb = 0.45$	$M = 0.65$	$Ub = 0.9$
$Lb = 0.6$	$M = 0.8$	$Ub = 1.0$

It can be seen from Tables 4–6 that the influence between parameters and the weight of parameters could significantly affect the ranking results. A parameter will absolutely rank the last if the weight of this parameter is 0.

4.4.2. Sensitivity analysis used in uncertainty source identification

Comparing the uncertainty results which used the existing sensitivity analysis method, the uncertainty results utilized the EFAST-based sensitivity analysis method.

It is shown in Fig. 4. Both the mean and the variance of current method were smaller than the original method. The mean of the EFAST-based method was closer to the mean of simulation result, and the variance decreasing means implies that the result was more stable.

The top two/four/all KFS were selected as the model inputs according to Table 2. The result is shown in Fig. 5.

It can be seen from Figs. 4 and 5:

1) The number of chosen KFS grows and the variance of the N_f probability distribution is larger.
2) The difference between four KFS results and two KFS results is much smaller than the difference between four KFS results and all KFS results.
3) Increasing the number of KFS in a confidence interval without a significant increase of variance, the result is much closer to the reality. However, as the number of KFS has overcome some confidence intervals, the variance will increase significantly.

In real practices, the number of KFS is not the more the better. The advice is to choose the top 60% to 80% parameters and give up the other 20% to 40% parameters with low ranking. On the precondition of precision, it enhanced the reliability of the results.

4.4.3. Quantification of uncertainty sources

According to the conclusion of Section 4.4.2, the first three KFS were selected in the uncertainty identification and qualified by the envelope-probability method. The distribution type and the range of the parameters are shown in Table 7.

For example, the possible values of solder joint thermal fatigue parameters are listed in Table 8 classified by different distribution types.

Simplifying the equation of the solder joint thermal fatigue, we have the following [16]:

$$N_f = \frac{1}{2}\left[\frac{0.7185 \times {L_D}^2}{\varepsilon_f \times h}\right]^{-2.27}. \tag{12}$$

The envelope-probability area of each KFS is shown in Fig. 6.

According to Eq. (12), in combination with the values in Table 4, *Area B* is 255.1661, which is shown in Fig. 7.

Then using each set of Table 8 as the value of ε_f to cut the envelope-probability area, the *Area* T_1, *Area* T_2, and *Area* T_3 can be painted as Fig. 8.

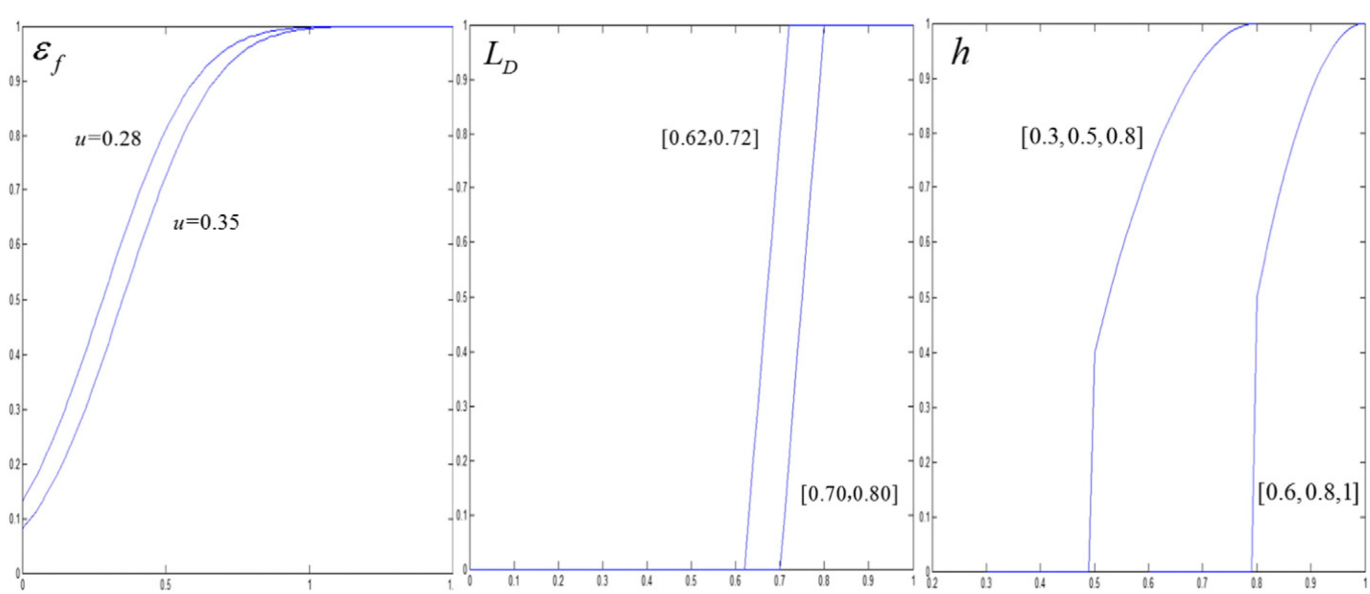

Fig. 6. The envelope-probability area of each KFS.

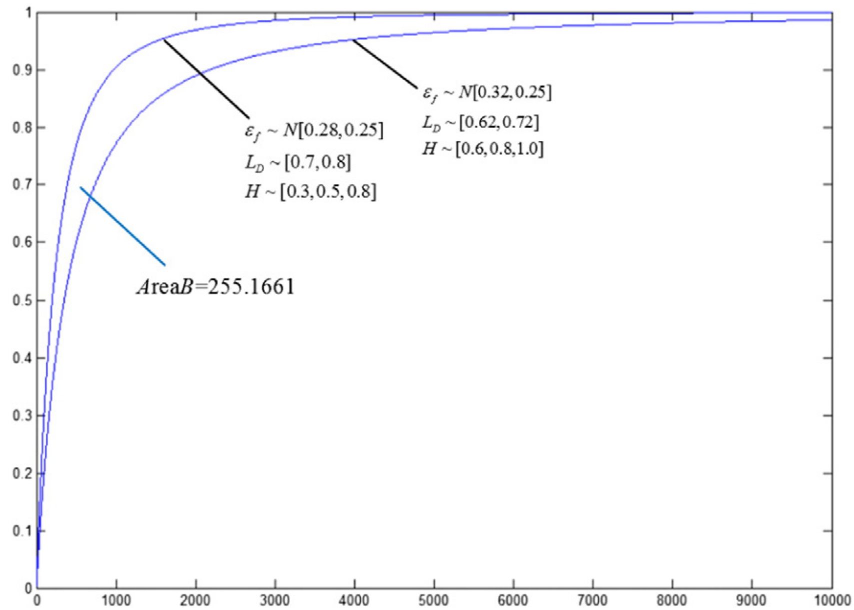

Fig. 7. The total envelope-probability area.

According to Eq. (11), $\Delta s_1 = 56.9\,\%$, $\Delta s_2 = 35.7\,\%$, and $\Delta s_2 = 52.2\,\%$, when the Δs_i is smaller than others, the impact of the ε_f fluctuation is greater and thus, $\varepsilon_f \sim [0.28, 0.25]$. The quantification results of the rest KFS are shown in Table 9.

4.4.4. Sensitivity analysis used in the quantification of uncertainty sources

Calculating the results of electronic prognostic uncertainty quantification.

It can be seen from Fig. 9:

1) The mean of the uncertainty quantification that used the envelope-probability based sensitivity analysis is 1367, and the variance is 312. Both the mean and the variance of current method were smaller than those resulted in Section 4.4.2. It indicates that the sensitivity analysis in the quantification of uncertainty sources can improve the accuracy of uncertainty quantification.
2) If the sensitivity of a KFS to results is higher than others, the distribution parameters of it will affect the outputs more greatly.

5. Conclusion

In this paper, the sensitivity analysis was conducted in the inputs of uncertainty quantification. First of all, the EFAST-based sensitivity method was utilized in KFS identification. The result of the EFAST-based method showed that it improved the accuracy and stability of the uncertainty quantification. This paper also tried to propose a method about how to choose the number of KFS. The key was to control the variance and meanwhile adhere to the simulation result. Secondly, the envelope probability-based sensitivity method was used in the KFS quantification. The result of the envelope-probability-based method showed that it further improved the accuracy and stability of

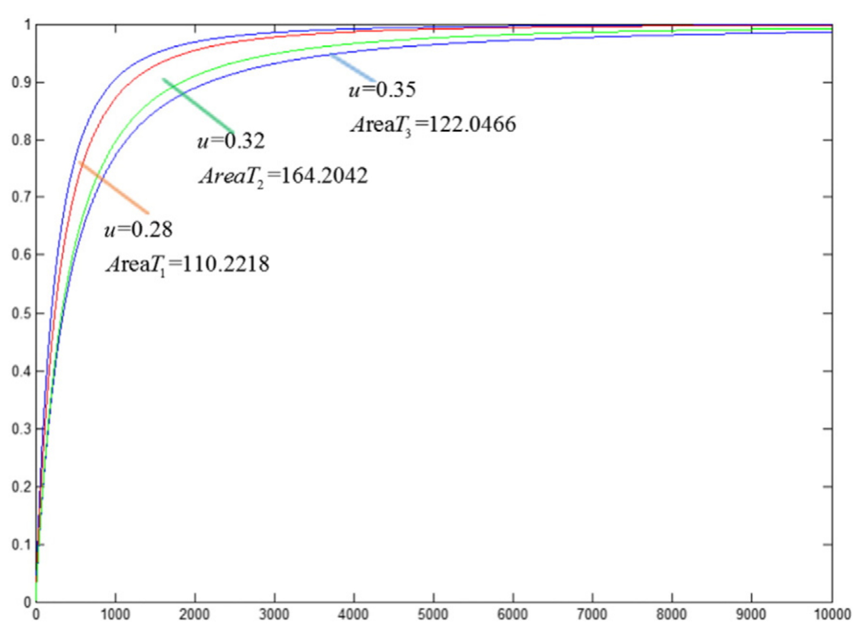

Fig. 8. The results of the envelope-probability area cut.

Table 9
The results of the qualification of the KFS.

Parameters	Range of the parameters		
ε_f	$u = 0.28$		$\sigma^2 = 0.25$
E_{Cu}	$u = 1350$		$\sigma^2 = 450$
d	$u = 0.7$		$\sigma^2 = 0.6$
L_D	$Lb = 0.62$		$Ub = 0.72$
t	$Lb = 0.15$		$Ub = 0.35$
l	$Lb = 0.5$		$Ub = 0.8$
W	$Lb = 0.05$		$Ub = 0.12$
h	$Lb = 0.5$	$M = 0.7$	$Ub = 1.0$
j	$Lb = 2.8$	$M = 3.2$	$Ub = 3.5$

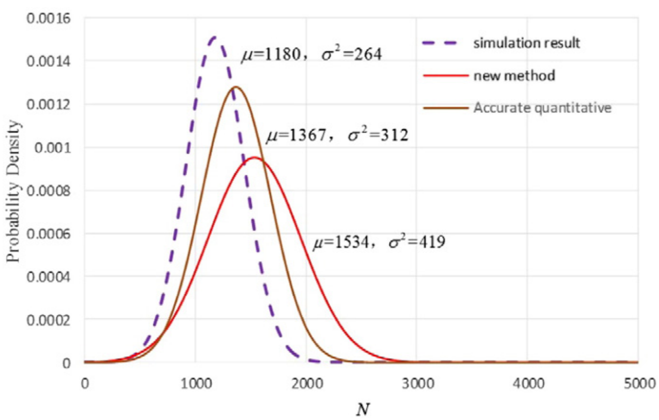

Fig. 9. The results of the envelope-probability based method.

the uncertainty quantification. Finally, this paper still has much room for further improvement. In the process of KFS identification, the scale of the weighting parameters can be set to 0.1 or even smaller. In the process of KFS quantification, the range of possible values can be divided into 10 groups. Such changes were more likely to further improve the accuracy and stability of the uncertainty quantification. However, it cost more calculation time than before. Therefore, how to balance time and accuracy can be further studied in the future.

References

[1] M. Pecht, Prognostic and Health Management of Electronics, John Wiley & Sons, Ltd., 2008.

[2] L. Vezzaro, P.S. Mikkelsen, Application of global sensitivity analysis and uncertainty quantification in dynamic modelling of micro pollutants in storm water runoff, Environ. Model Softw. 27 (2012) 40–51.

[3] S. Kucherenko, B. Feil, N. Shah, et al., The identification of model effective dimensions using global sensitivity analysis, Reliab. Eng. & Syst. Saf. 96 (4) (2011) 440–449.

[4] J. Jung, N. von der Assen, A. Bardow, Sensitivity coefficient-based uncertainty analysis for multi-functionality in LCA, Int. J. Life Cycle Assess. 19 (3) (2014) 661–676.

[5] B. Vo, S. Singh, A. Doucet, Sequential Monte Carlo methods for multitarget filtering with random finite sets, IEEE Trans. Aerosp. Electron. Syst. 41 (4) (2005) 1224–1245.

[6] S. Sankararaman, S. Mahadevan, Bayesian methodology for diagnosis uncertainty quantification and health monitoring, Struct. Control. Health Monit. 20 (1) (2013) 88–106.

[7] J.C. Helton, J.D. Johnson, W.L. Oberkampf, A sampling-based computational strategy for the representation of epistemic uncertainty in model predictions with evidence theory, Comput. Methods Appl. Mech. Eng. 196 (37) (2007) 3980–3998.

[8] T. Andre, Practical strategies for sensitivity analysis given models with large parameter sets, Proceedings of the International Workshop on Uncertainty, Sensitivity, and Parameter Estimation for Multimedia Environmental Modeling 2003, pp. 81–82.

[9] A. Ligmann-Zielinska, Spatially-explicit sensitivity analysis of an agent-based model of land use change, Int. J. Geogr. Inf. Sci. 27 (9) (2013) 1764–1781.

[10] G. Li, C. Rosenthal, H. Rabitz, High-dimensional model representations, J. Phys. Chem. 105 (33) (2003) 7765–7777.

[11] J.C. Helton, F.J. Davis, Latin hypercube sampling and the propagation of uncertainty in analyses of complex systems, Reliab. Eng. Syst. Saf. 81 (3) (2003) 23–69.

[12] A. Saltelli, S. Tarantola, K.P.S. Chan, A quantitative model-independent method for global sensitivity analysis of model outputs, Technimetrics 41 (1) (1999) 39–56.

[13] J.S. Hammonds, F.O. Hoffman, S.M. Bartell, An Introductory Guide to Uncertainty Analysis in Environmental and Health Risk Assessment, US DOE, 1994.

[14] Scott Ferson, W. Troy Tucker, Sensitivity analysis using probability bounding, Reliab. Eng. Syst. Saf. 91 (11–12) (2006) 1435–1442.

[15] Bo Sun, Shengkui Zeng, Rui Kang, M.G. Recht, Benefits and challenges of system prognostic, IEEE Trans. Reliab. (61) (2012) 323–335.

[16] V. Gektin, A. Bar-Cohen, S. Witzman, Coffin–Manson based fatigue analysis of under filled DCAs, IEEE Trans. Compon. Packag. Manuf. Technol. Part A 21 (4) (1998) 577–584.

[17] C. F., I. C. U., D.L. M., Thermal stress and fatigue analysis of plated-through holes using an internal state variable constitutive model, Finite Elem. Anal. Des. 30 (1) (1998) 1–17.

[18] P- Wang, G.S. Cargill, I.C. Noyan, et al., Electro migration-induced stress in aluminum conductor lines measured by x-ray micro diffraction, Appl. Phys. Lett. 72 (11) (1998) 1296–1298.

[19] D. Cong, A Probabilistic Linear Cumulative Damage Rule for Predicting Fatigue Life, J. Northwest. Polytech. Univ. (1993) (2:004).

[20] A.R. McLean, M.M. Rosado, F. Agenes, et al., Resource competition as a mechanism for B cell homeostasis, Proc. Natl. Acad. Sci. 94 (11) (1997) 5792–5797.